

BASIC SCIENCES



Turbulent Flow Promotes Cleavage of VWF (von Willebrand Factor) by ADAMTS13 (A Disintegrin and Metalloproteinase With a Thrombospondin Type-1 Motif, Member 13)

Maria Bortot, Katrina Ashworth, Alireza Sharifi, Faye Walker, Nathan C. Crawford, Keith B. Neeves, David Bark Jr, Jorge Di Paola

OBJECTIVE—Acquired von Willebrand syndrome is defined by excessive cleavage of the VWF (von Willebrand Factor) and is associated with impaired primary hemostasis and severe bleeding. It often develops when blood is exposed to nonphysiological flow such as in aortic stenosis or mechanical circulatory support. We evaluated the role of laminar, transitional, and turbulent flow on VWF cleavage and the effects on VWF function.

APPROACH AND RESULTS—We used a vane rheometer to generate laminar, transitional, and turbulent flow and evaluate the effect of each on VWF cleavage in the presence of ADAMTS13 (a disintegrin and metalloproteinase with a thrombospondin type-1 motif, member 13). We performed functional assays to evaluate the effect of these flows on VWF structure and function. Computational fluid dynamics was used to estimate the flow fields and forces within the vane rheometer under each flow condition. Turbulent flow is required for excessive cleavage of VWF in an ADAMTS13-dependent manner. The assay was repeated with whole blood, and the turbulent flow had the same effect. Our computational fluid dynamics results show that under turbulent conditions, the Kolmogorov scale approaches the size of VWF. Finally, cleavage of VWF in this study has functional consequences under flow as the resulting VWF has decreased ability to bind platelets and collagen.

CONCLUSIONS—Turbulent flow mediates VWF cleavage in the presence of ADAMTS13, decreasing the ability of VWF to sustain platelet adhesion. These findings impact the design of mechanical circulatory support devices and are relevant to pathological environments where turbulence is added to circulation.

VISUAL OVERVIEW: An online [visual overview](#) is available for this article.

Key Words: aortic valve stenosis ■ collagen ■ hemostasis ■ von Willebrand Factor

VWF (von Willebrand Factor) is a large multimeric protein that plays an essential role in primary hemostasis by mediating platelet adhesion to subendothelial collagen and by supporting platelet-platelet interactions at high shear rates under controlled experimental conditions.^{1,2} The capacity for VWF to sustain hemostasis relies on its force-dependent conformation.^{3–5} VWF circulates in an inactive globular form, and sufficient mechanical forces cause a conformational change to an extended form^{6,7} that exposes 3 domains that are critical for its function. The A1 domain mediates binding to the platelet GPIIb- α (glycoprotein IIb- α) and integrin $\alpha_{IIb}\beta_3$ receptors. The A2 domain exhibits the cryptic Tyr¹⁶⁰⁵-Met¹⁶⁰⁶ cleavage site,

See accompanying editorial on page 1702

and the A3 domain mediates binding to collagen.⁸ The precise step-by-step process of VWF elongation and sequential exposure of its domains is not fully understood. The fluid mechanical forces required for exposure of each domain has been reported.^{9–12} The magnitude of the forces required for exposure seems to depend on whether VWF is tethered to collagen and its multimer size. In addition, the threshold for initial elongation might have limited physiological significance, as elongation alone is not sufficient for GPIIb- α binding.¹² VWF's primary protease ADAMTS13 (a disintegrin and metalloproteinase with a thrombospondin

Correspondence to: Jorge Di Paola, MD, University of Colorado School of Medicine, 12800 E, 19th St, Aurora, CO 80045. Email jorge.dipaola@ucdenver.edu

The online-only Data Supplement is available with this article at <https://www.ahajournals.org/doi/suppl/10.1161/ATVBAHA.119.312814>.

For Sources of Funding and Disclosures, see page 1840.

© 2019 American Heart Association, Inc.

Arterioscler Thromb Vasc Biol is available at www.ahajournals.org/journal/atvb

Nonstandard Abbreviations and Acronyms

ADAMTS13	a disintegrin and metalloproteinase with a thrombospondin type-1 motif, member 13
Ag	antigen
AS	aortic stenosis
AVWS	acquired von Willebrand syndrome
GPIb-α	glycoprotein Ib- α
HMWM	high molecular weight multimers
HSA	human serum albumin
MCS	mechanical circulatory support
Re	Reynolds Number
RSS	Reynolds Shear Stress
VAD	ventricular assist device
VWF	von Willebrand factor

type-1 motif, member 13) is constitutively active,¹³ but its proteolytic activity is regulated by VWF conformation.

VWF's hemostatic capacity is dependent on its multimeric structure.¹⁴ The mature molecule is comprised of ultra large, high molecular weight multimers (HMWMs), medium and low molecular weight multimers. Larger multimers have greater hemostatic capacity, presumably because they require lower shear stress to elongate,^{11,15} which exposes the A1 domain for platelet adhesion. VWF is stored in platelet α granules and in Weibel-Palade bodies of endothelial cells. In a regulated process, VWF is secreted from endothelial cells in the ultra large molecular weight multimers form, which is rapidly cleaved by ADAMTS13. Since ultra large molecular weight multimers readily bind platelets,¹⁶ reduced VWF cleavage either by congenital deficiency or antibody-mediated inhibition of ADAMTS13 promotes microthrombi in the microvasculature, hemolysis, and thrombocytopenia¹⁷ causing thrombotic thrombocytopenic purpura.¹⁸ Conversely, excessive VWF cleavage causes reduced platelet adhesion and bleeding complications, as seen in von Willebrand disease type 2A.¹⁹

Acquired von Willebrand syndrome (AVWS)²⁰ is characterized by the loss of HMWM and is often associated with nonphysiological blood flows.^{21,22} AVWS can be found in individuals with severe aortic stenosis (AS), those undergoing cardiopulmonary bypass, or following left ventricular assist device implantation. In this article, we refer to these different heart assist devices as mechanical circulatory support (MCS) devices. Bleeding in these situations is highly variable with reports of excessive bleeding ranging from 20% to 60% in affected patients.^{23–26} Though many of these patients are taking anticoagulants, the bleeding in this setting is usually more pronounced than expected, suggesting a potential role for dysfunctional VWF.²⁷ As full recovery of VWF levels and multimer composition occur after physiological flow is restored (eg, post-aortic valve replacement or device removal), it has been suggested that

Highlights

- High shear stress in the presence of ADAMTS13 (A Disintegrin and Metalloproteinase With a Thrombospondin Type-1 Motif, Member 13) is not sufficient for excessive cleavage of VWF (von Willebrand Factor).
- Turbulence as seen in aortic stenosis and mechanical recirculation devices, in the presence of ADAMTS13, mediates excessive cleavage of VWF.
- Excessively cleaved VWF is functionally deficient and cannot sustain robust platelet and collagen adhesion.

nonphysiological blood flow plays a role in causing VWF cleavage.^{28–30} However, the specific features of blood flow that cause VWF elongation, with subsequent excessive cleavage by ADAMTS13^{31,32} have not been fully identified.

Previously, the conditions that modulate VWF-ADAMTS13 interactions have been studied using a vortex-based assay that generate relatively high shear stress and chaotic fluid patterns within a polymerase chain reaction tube.^{33–36} This vortex approach results in VWF cleavage and has identified cofactors that augment VWF cleavage that otherwise cannot be tested in the presence of denaturants.³⁷ Specifically, studies suggest that flow conditions within the vortex assay mediate cleavage, but little is known about the fluid characteristics involved because flow in vortexers is difficult to quantify.

Fluid flow can be categorized into 3 regimes: laminar, transitional, or turbulent. Under laminar conditions, the flow is characterized by smooth, generally parallel, pathlines and can be described as having a highly ordered motion, whereas under turbulent conditions it exhibits velocity fluctuations and highly disordered motion (flow is chaotic with eddies that are involved with the transfer energy across many scales).^{38,39} Transitional flow is partly laminar and partly turbulent, it contains a disordered dynamic multidirectional flow component that is superimposed over well-ordered flow.⁴⁰ The transition between laminar and turbulent flow depends on the Reynolds number (Re), a nondimensional parameter that represents the ratio of inertial forces to viscous forces. As the flow velocity increases, that is, the Re increases, the inertial forces dominates the viscous forces.⁴¹ The transition from laminar to turbulent flow occurs when the inertial force become so significant that the viscous force is no longer able to dampen the scattered disturbances in the flow on the macroscale.⁴¹ Turbulent flows have been shown to occur in MCS devices and severe AS,^{42–46} whereas most studies on VWF are conducted under laminar flow conditions.⁴⁷ VWF cleavage assays conducted under laminar conditions at high shear stress magnitudes can provide insights about physiological cleavage of VWF by ADAMTS13. Physiological cleavage is responsible for the heterogeneous distribution of VWF

molecules reported in plasma from healthy patients.⁴⁸ However, the fluid forces leading to excessive and pathological cleavage of VWF are still unknown.

We hypothesized that turbulent flow plays role in excessive cleavage of VWF by ADAMTS13 beyond what is seen by high shear stress and renders the VWF molecule incapable of sustaining platelet adhesion. To test this hypothesis, we used a rotational shear rheometer to explore the effects of these nonphysiological fluid forces on VWF cleavage and function under highly controlled flow conditions that include laminar, transitional, and turbulent flows.

METHODS

The data that support the findings of this study are available from the corresponding author on reasonable request. Details of the major resources can be found in the [online-only Data supplement](#).

Blood Collection

Blood collection was conducted in accordance with the Declaration of Helsinki and the Institutional Review Board of the University of Colorado, Anschutz Medical Campus. Blood was drawn after informed consent was obtained from healthy donors (males between 30 and 50 years old) by venipuncture into 4.5-mL vacutainer tubes containing 3.2% sodium citrate. An initial tube was discarded to avoid any influence on platelet activation from the initial puncture. Samples were used within 90 minutes of phlebotomy. Before the assay, blood was recalcified as previously described.⁴⁹

Recombinant ADAMTS13 Measurement

Recombinant ADAMTS13 was obtained from previously transfected HEK-293 cell supernatants.⁵⁰ Cell supernatant containing ADAMTS13 was collected and filtered. ADAMTS13 activity was measured using the fluorescence resonance energy transfer assay that contains a synthetic 73-amino-acid residues of VWF from D1596 to R1668 (FRETS-VWF73, Peptides International, KY) used to measure the protease activity based on the method described by Kokame et al.⁵¹ Briefly, varying volumes of samples containing ADAMTS13 were diluted in reaction buffer before being added to a 96-well plate. Subsequently, the fluorescence-quenching substrate for ADAMTS13 was added. Fluorescence of each well was measured every 5 minutes for 90 minutes on a plate reader (Synergy 2, BioTek). Values were established by comparing them to a standard curve determined by measuring pooled plasma from healthy controls.

Vortex Method of VWF Cleavage

A standard cleavage product, used as a positive control, was prepared as previously described^{37,52} with modifications. Recombinant human VWF (Vonvendi) and ADAMTS13 were incubated for 1 hour at varying concentrations in a 96-well plate. Wells were blocked with 30 mg/mL HSA (human serum albumin) in PBS solution for 2 hours. Then, 30 μ g/mL VWF, 2.5 U/mL ADAMTS13 were added to the wells and placed on a vortexer (VWR Standard Microplate Vortex Mixers, VWR) for 30 minutes at a speed of 7 (estimation from VWR Vortex

Mixer manual: 1540 rpm). VWF antigen (Ag) was measured by ELISA. As previously described,⁵³ the anti-VWF monoclonal antibodies AVW-1 and 105.4 (BloodCenter of Wisconsin) were used for capture. The detection was conducted using a rabbit-antihuman VWF pAb (Dako, Carpinteria, CA), and a HRP (horseradish peroxidase)-conjugated goat-anti-rabbit antibody (Bio-Rad Laboratories, Hercules, CA). Absorbance was read at 450 nm in a plate reader (Synergy 2, BioTek).

Vane Rheometer Studies of VWF Cleavage

Cleavage experiments were conducted using a HAAKE MARS 60 rheometer (Thermo Fisher Scientific) equipped with a 4-blade vane rotor (FL16; diameter: 16 mm, length: 8.8 mm, material: titanium) and a stainless steel cup (CCB26; diameter: 27.2 mm). To accommodate a sample volume of only 7 mL, the axial gap between the vane blades (1 mm thick) and the bottom of the cup was set to 1 mm (Figure 1A and 1B). Temperature was controlled with the Peltier temperature module set to 21°C. Figure 1A and 1B shows complete dimensional specifications for the vane setup. In short, 7 mL of buffer containing 30 μ g/mL VWF, 2.5 U/mL ADAMTS13, 30 mg/mL HSA dissolved in PBS solution was placed in the cup completely covering the vane. The rotation rate of the rheometer was increased until a critical speed was reached where the fluid no longer exhibited a linear torque response and the measured torque began to increase nonlinearly. This change in torque indicates the transition between well-defined laminar flow ($Re < Re_c$), where Re_c is critical Reynolds Number, and the onset of secondary flows ($Re > Re_c$).⁵⁴ As the rotation rate was further increased, a second transition was observed where the measured torque increased drastically signifying the onset of turbulent flow. The set rotation rates and resultant torque values were not converted to rheological parameters, shear stress, and shear rate, respectively because assumptions that relate the 2 through analytical calculations in the vane rheometer are no longer valid when the flow is not laminar ([online-only Data Supplement](#)).

Cone-and-Plate Rheometer Studies of VWF Cleavage

Cleavage experiments were conducted using a cone-and-plate rheometer equipped with a 40 mm diameter, 2° cone (DHR-2, TA Instruments). The temperature was maintained at 21°C via a Peltier temperature controller. Surfaces were blocked for 2 hours with 30 mg/mL HSA, and then a 50 μ L sample consisting of 30 μ g/mL VWF, 2.5 U/mL ADAMTS13, and 30 mg/mL HSA dissolved in PBS solution was added. Tests were conducted for 0.5, 1, 5, and 10 minutes at shear rates of 1000 to 7000 sec^{-1} . Note that the cone-and-plate rheological results were only in laminar flow, corresponding to a linear relationship between shear stress and shear rate ([online-only Data Supplement](#)).

Western Blotting

Samples were subjected to 3% to 8% SDS-PAGE and transferred to polyvinylidene difluoride membranes (Invitrogen). Membranes were blocked for 1 hour and then incubated with a rabbit-anti-human polyclonal VWF (Dako, Carpinteria, CA). All incubation and washing steps were performed at room temperature in 5% nonfat dry milk. After 3 washing steps, they were incubated for 1 hour with a HRP-conjugated goat-anti-rabbit

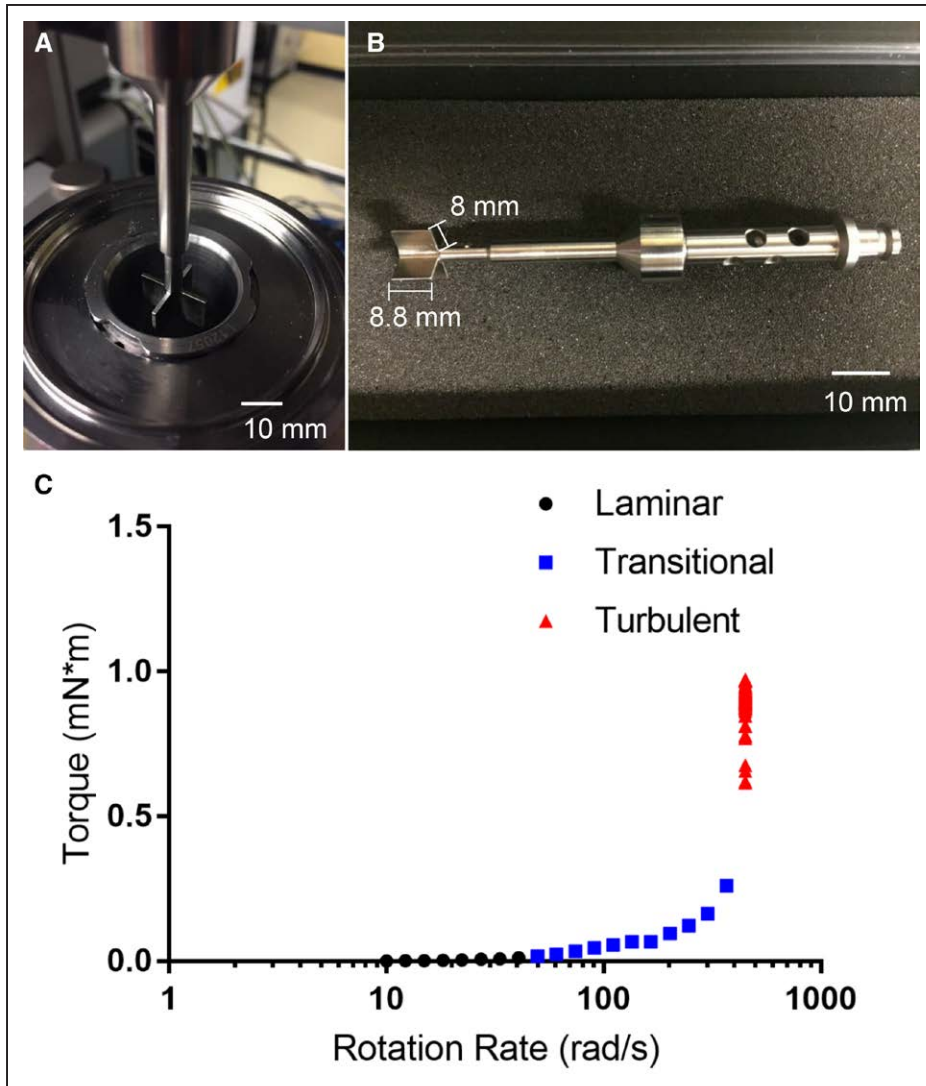


Figure 1. Vane and cup rheological setup.

A, Top view of the vane setup, which consists of a 4-blade vane rotor that is lowered into a stainless steel cup (internal radius of 13.6 mm) until a 1 mm axial gap between the vane and the bottom of the cup is achieved. **B**, Side view of the vane rotor, which consists of 4 blades with a 1 mm thickness. **C**, Measured torque as a function of input rotational rate showing the determination of laminar, transitional, and turbulent flow regimes.

antibody (Bio-Rad Laboratories, Hercules, CA). Subsequently, membranes were developed with Western Lightning-ECL (Perkin Elmer, Waltham, MA), and bands were visualized by exposure to Fujifilm Super RX (Edison, NJ). Uncleaved VWF was detected with the presence of a 225-kDa band whereas cleavage fragments were detected with the presence of a 176- and 140-kDa bands as previously reported.^{55,56}

VWF Multimer Analysis

SDS-agarose gel electrophoresis was performed as previously described.⁵⁷ Briefly, low resolution gels (1.2%) were prepared (HGT agarose, Lonza, Rockland, ME), and 1 mU VWF from each sample was added to each lane. Electrophoresis was conducted for 16 hours at 45 V. VWF multimers were then transferred to an Immobilon-P (Millipore, Billerica, MA) membrane at 4°C in transfer buffer (25 mmol/L Tris, 200 mmol/L glycine, 20% methanol, and 0.03% SDS). Western blotting

and densitometry were performed on the gels as previously reported.⁵⁸ Average size of multimers was estimated using a previously reported approach ([online-only Data Supplement](#)).⁵⁰

Collagen-Binding Assay

ELISA plates (Nunc-Immuno Maxisorp; Nunc A/S, Roskilde, Denmark) were coated with 1 µg/mL human type III collagen (Southern Biotech, Birmingham, AL) diluted in a calcium carbonate buffer and incubated at 4°C overnight. The plate was then washed and blocked with a 1% BSA solution for an hour before the samples were added at various dilutions and left to incubate for an hour. The plate was then washed, and samples were incubated with a rabbit-anti-human VWF pAb (Dako, Carpinteria, CA) before a wash and the addition of a HRP-conjugated goat-anti-rabbit antibody (Bio-Rad Laboratories, Hercules, CA). Absorbance was read at 450 nm in a plate reader (Synergy 2, BioTek). Collagen-binding ratio was calculated by evaluating

the ratio between collagen-binding and VWF Ag levels. This ratio represents the biological capacity of the available VWF to bind to collagen. As in prior studies,⁵⁹ we calculated ratios of VWF:collagen binding/VWF:Ag with normal defines as ≥ 0.7 .

VWF Activity and Ag

An automated latex enhanced immunoassay (HemosIL, Diagnostica Stago, France) was used to determine VWF activity (VWF:Act). This assay is based on the ability of VWF to bind GPIIb- α . Standard curves were prepared, and sample was added to the cuvettes required for the Compact Max (Diagnostica, Stago). At the same time, an immunoturbidimetric assay (LIATEST VWF:Ag, Diagnostica Stago, France) was performed according to the instructions of the manufacturer to determine the VWF Ag levels (VWF:Ag). The VWF:Act/VWF:Ag ratio was calculated and used to evaluate VWF activity.

Platelet Adhesion Flow Assay

A platelet adhesion flow assay was designed to identify possible functional changes in VWF from samples treated in the vane rheometer. A polydimethylsiloxane device containing circular wells (diameter: 4.5 mm) was used to pattern the capture of an anti-VWF monoclonal antibody (AVW-1, BloodCenter of Wisconsin) that binds the C-terminus of VWF. Subsequently, the wells were rinsed and blocked for 1 hour with 1% BSA buffer. Samples containing VWF (5 $\mu\text{g}/\text{mL}$) were added to each well, incubated for 1 hour, and rinsed and blocked again. Incubation was all done at room temperature. Then, the buffer was removed and a microfluidic device with channels of 12.5 μm high, 350 μm wide, 8000 μm long was placed over the patterned VWF. A phycoerythrin anti-human CD41 antibody (BioLegend, San Diego, CA) was used to label lyophilized platelets (Bio/Data Corporation, Horsham, PA) at a concentration of 6×10^8 platelets per milliliters. Lyophilized platelets do not allow granule release and, therefore, eliminate any effects from platelet endogenous VWF. These platelets were perfused through the channels for 5 minutes at a wall shear rate of 1800 second^{-1} near the central axis of the coverslip wall using a syringe pump (Harvard Apparatus) in withdraw mode. Platelet adhesion was visualized using an inverted microscope (Olympus IX-81, Olympus America, Center Valley, PA), and data were recorded every second using a 40 \times (numerical aperture, 0.6) objective on the region of interest using a high-speed camera (Hamamatsu Digital Camera, C11440, Orca-Flash 4.0). Platelet binding was quantified by counting individual adhered platelets per frame using an automated protocol developed in Fiji (ImageJ, National Institutes of Health). Image processing consisted of using several in-built ImageJ routines in sequence. Images were converted to grayscale; a threshold was applied followed by an in-built ImageJ edge finding routine. Images were then analyzed, and platelets were identified using size and circular geometry filters. Appropriate implementation of the image processing protocol was confirmed by using overlays to ensure the data being captured were correct and examples are shown on [online-only Data Supplement](#)

Computational Fluid Dynamics Analysis of the Vane Rheometer

The fluid in the vane rheometer was assumed incompressible and isothermal. The Reynolds Stress Model was used to

simulate turbulence in the vane rheometer using ANSYS 18.1. Geometry for the simulation was based on the FL16 4B/SS vane rotor and the CCB26 metal cup reported in Figure 1. A no-slip boundary condition was imposed on solid surfaces with vanes rotating with an angular velocity 10, 100, or 450 rad/second. A 0 velocity condition was applied everywhere along the cup, whereas symmetry was specified at the free surface. A mesh refinement analysis was carried out to ensure that the numerical solutions are independent of the mesh resolution. The mesh elements were tetrahedral and triangular, resulting in a total of over 750 000 elements.

Statistical Analysis

Statistical analyses were performed with GraphPad Prism 7.03 (GraphPad, La Jolla, CA). Significance was determined using a nonparametric ANOVA (Kruskal-Wallis test) with Dunn post hoc test was used to compare platelet binding at 100 seconds, VWF:collagen binding/VWF:Ag and VWF:Activity/VWF:Ag. All data are presented as the mean \pm SE unless otherwise noted. All assays were conducted in triplicate.

RESULTS

Defining Flow Regimes in a Vane Rheometer

To test the hypothesis that turbulent flow may potentiate VWF cleavage, we turn to a vane rheometer (Figure 1A and 1B) and define the following flow regimes for a Newtonian fluid: laminar flow is defined by linear response between the torque and rotation rate. Transitional flow is defined by the onset of a nonlinear response between torque and rotation rate. Turbulent flow is defined by an asymptote in the torque and a critical rotation rate. The purified system of VWF, HSA, and ADAMTS13 is a Newtonian fluid ([online-only Data Supplement](#)) that is its viscosity is not a function of shear rate. Laminar flow was observed at rotation rates from 10 to 40 rad/second, where the torque steadily increased as a function of increasing rotation rate (Figure 1C). Transitional flow was observed at rotation rates of 40 to 400 rad/second as the torque signal deviated from the initial linear behavior. Finally, turbulent flow was observed at rotation rates >400 rad/second.

Turbulent Flow in a Vane Rheometer Supports VWF Cleavage

The effect of laminar (10 rad/second), transitional (100 rad/second), and turbulent (450 rad/second) flow on VWF cleavage by ADAMTS13 was evaluated using the vane rheometer. Like in prior VWF cleavage studies,⁶⁰ samples were exposed to the flow regime for 10 minutes. Results evaluated through western blots show VWF cleavage, as indicated by 176- and 140-kDa bands, only under turbulent flow conditions (Figure 2A). To evaluate the impact of exposure time, the experiment was repeated for 30 minutes; cleavage and nearly full digestion of

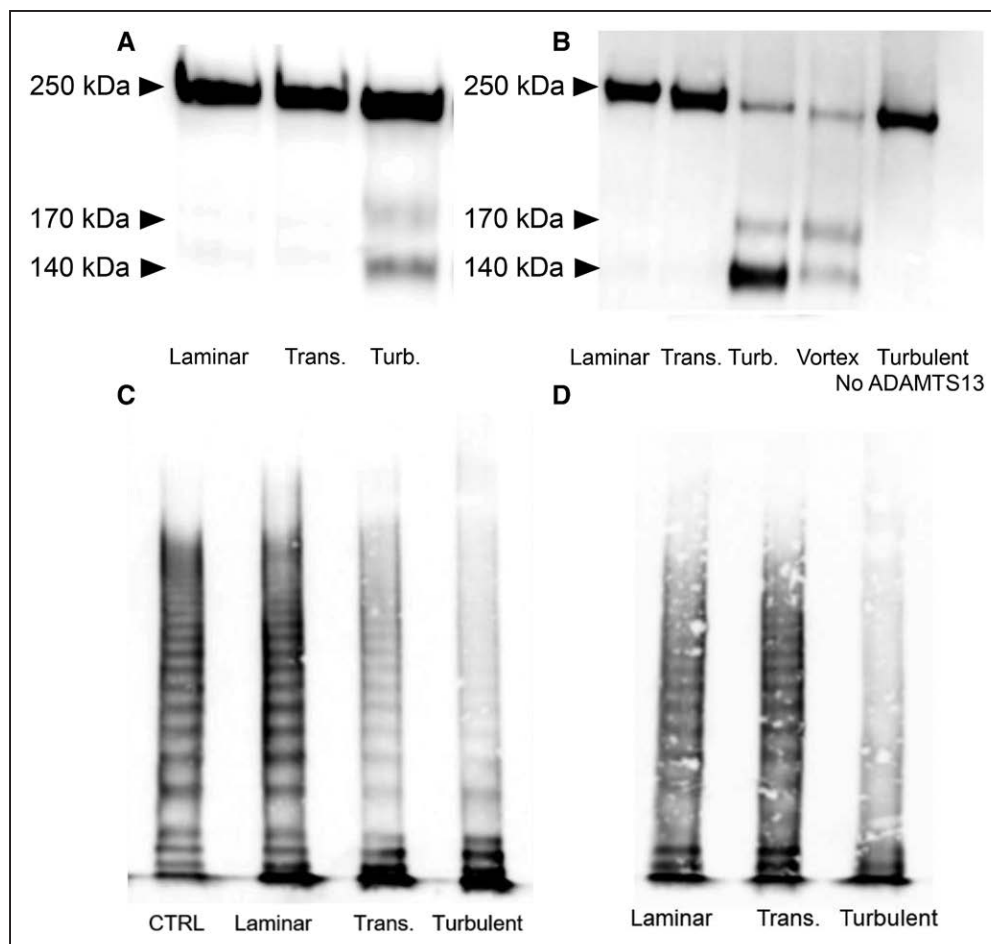


Figure 2. Western blot and multimer analysis.

Results comparing cleavage under laminar, transitional, and turbulent flows. **A**, Representative image of western blot from samples tested in the vane rheometer for 10 min. All samples contained VWF (von Willebrand Factor) and ADAMTS13 (a disintegrin and metalloproteinase with a thrombospondin type-1 motif, member 13). Samples in the figure are representative of the samples subjected to (1) laminar conditions; (2) transitional condition, and (3) turbulent conditions for 10 min. **B**, Western Blot from VWF and ADAMTS13 samples after flow assay under varying flow regimes of samples exposed for 30 min. (1) Laminar flow, (2) transitional flow, (3) turbulent conditions, (4) vortex method (+control), (5) turbulent flow conditions in absence of ADAMTS13. **C**, Multimer analysis of samples exposed to control CTRL: un-sheared sample, laminar sample, transitional sample, and turbulent conditions for 30 min. **D**, Multimer analysis of blood samples tested. (1) Laminar flow, (2) transitional flow, and (3) turbulent conditions. Ag indicates antigen; and CB, collagen binding.

VWF was observed in samples subjected to turbulent flow (Figure 2B). No cleavage was detected in samples exposed to laminar and transitional flow. Similarly, loss of HMWV of VWF was evident in the sample exposed to turbulent flow at both time points and interestingly, albeit less evident, in samples exposed to transitional flow (Figure 2C; [online-only Data Supplement](#)). Cleavage was not observed on samples exposed to turbulent flow without ADAMTS13, indicating that cleavage was mediated by ADAMTS13 and not mechanical degradation. To investigate if the same cleavage occurs in the presence of blood cells and plasma, we performed experiments with whole blood. Whole blood samples subjected to turbulent conditions also showed loss of HMWV by multimer analysis (Figure 2D). These data demonstrate that turbulent conditions in a vane rheometer are sufficient to cause VWF cleavage in the presence of ADAMTS13 in purified and whole blood systems.

VWF Functional Deficits in Different Flow Regimes

To determine the functional consequences of excessive cleavage of VWF, we evaluated the protein's function following exposure to laminar, transitional, and turbulent flows by quantifying platelet adhesion under physiological shear rates (1800 second^{-1}) in a microfluidic device. As representative images shown on Figure 3A through 3D, platelet adhesion to VWF decreased from unstressed controls (Figure 3A) and as the flow transitions from laminar (Figure 3B), transitional (Figure 3C) to turbulent (Figure 3D). Adhesion of platelets to VWF exposed to control, laminar, and transitional flows increased with time reaching maximal adhesion at ≈ 100 seconds. Conversely, binding of platelets to VWF exposed to turbulent flow was minimal (Figure 3E). Platelet adhesion at 100 seconds under transitional and turbulent flows was significantly reduced when compared with the control

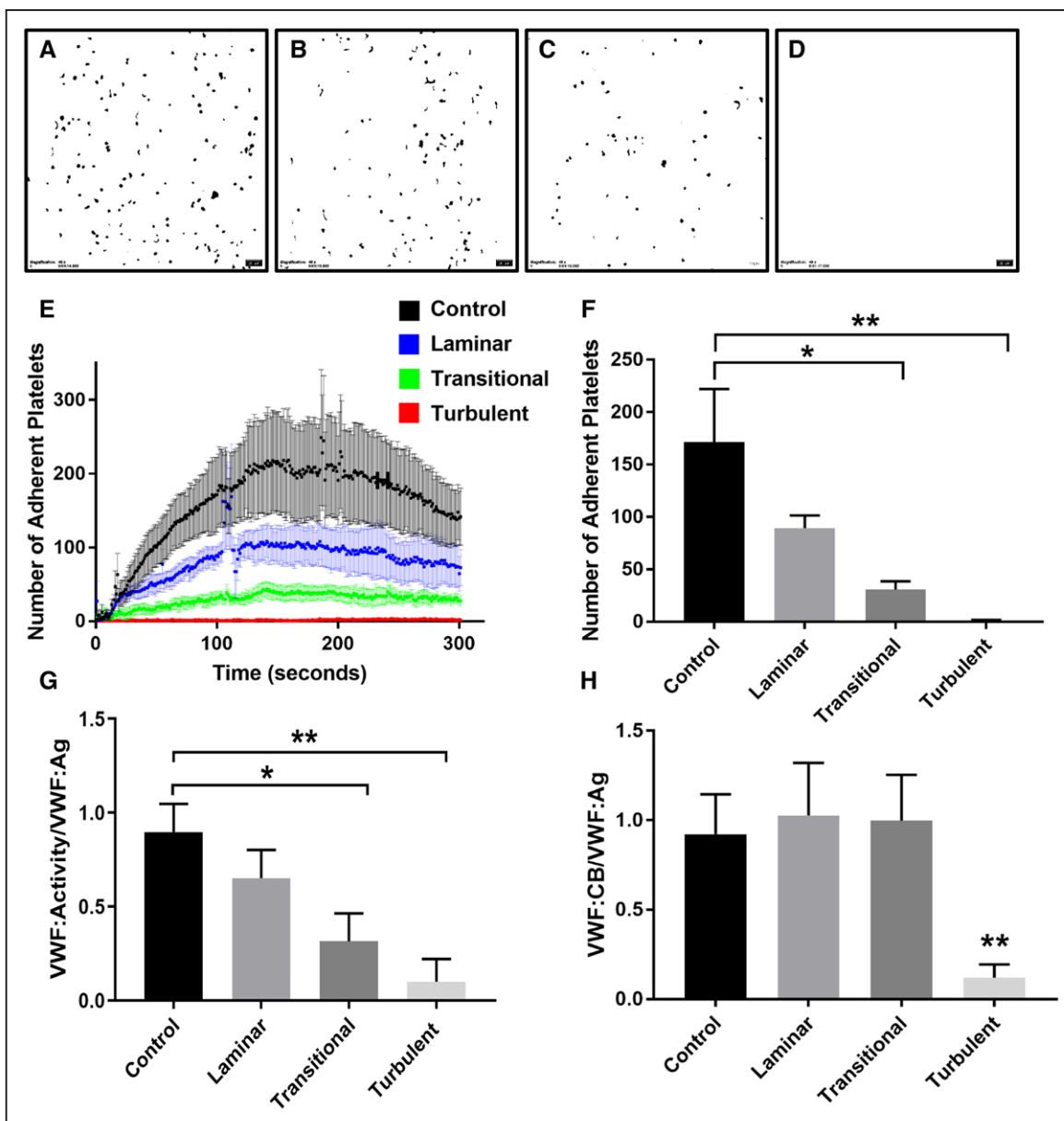


Figure 3. VWF (von Willebrand Factor) function post-exposure to laminar, transitional, and turbulent flows.

A, Control VWF: example of adherent platelets to control VWF. **B**, Laminar flow: example of adherent platelets to VWF previously subjected to laminar flow conditions. **C**, Transitional flow: example of adherent platelets to VWF previously subjected to transitional flow conditions. **D**, Turbulent flow: example of adherent platelets to VWF previously subjected to turbulent flow conditions. **E**, Number of adherent platelets over 300 seconds ($P < 0.001$). **F**, Number of adherent platelets at 100 s ($*P < 0.05$, $**P < 0.01$). **G**, VWF activity to VWF antigen (Ag) levels ($*P < 0.05$, $**P < 0.01$), for the turbulent sample, the VWF activity was ≤ 10 , the detection limit of the assay. **H**, Collagen-binding (CB) ratio ($*P < 0.05$, $**P < 0.01$).

(Figure 3F). However, although a trend in reduction of platelet adhesion was found, there was no statistically significant difference between the control and the VWF previously exposed to laminar conditions. Similarly, VWF activity was reduced in the samples exposed to transitional and turbulent conditions in an assay that measures the ability of VWF to bind the platelet receptor GPIIb- α (Figure 3G). Only the VWF sample exposed to turbulent conditions showed significant reduction of VWF ability to bind collagen (VWF:collagen binding/VWF:Ag) compared with controls (Figure 3H). These results suggest

that transitional flow has an effect on VWF function as shown by the impaired platelet binding and that turbulent flow causes even further reduction in VWF's ability to interact with GPIIb- α and collagen.

Flow Characteristics in the Vane Rheometer

As our results show that turbulent flow mediates excessive cleavage of VWF, we sought to further describe the flow patterns and forces in the vane rheometer using computational fluid dynamics. The experimental

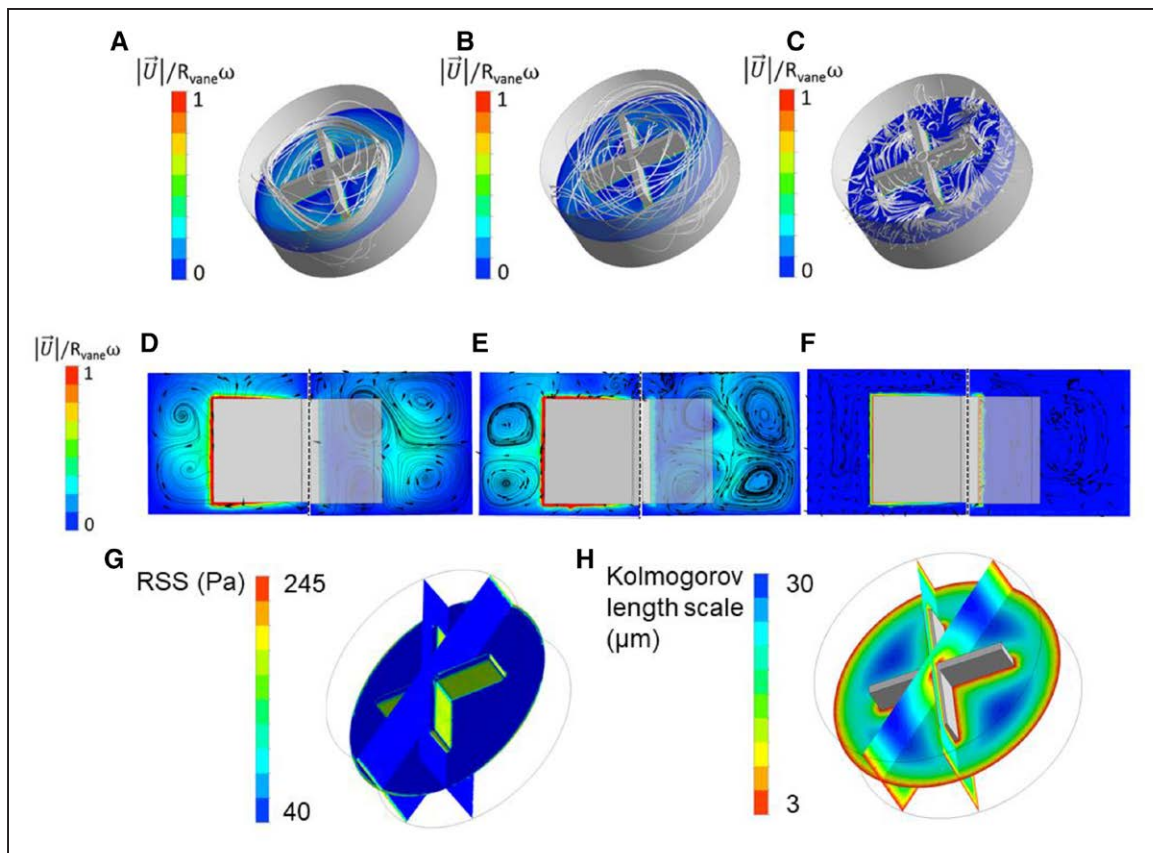


Figure 4. Computational fluid dynamics results showing 3-dimensional particle pathlines and velocity magnitude contours on the middle plane for the different rotating speeds.

A, 10 rad/s, **(B)** 100 rad/s, **(C)** 450 rad/s. **D**, Normalized velocity magnitude and pathlines on plane 1 (left) and plane 2 (right) for rotating speed 10 rad/s. **E**, Normalized velocity magnitude and pathlines on plane 1 (left) and plane 2 (right) for rotating speed 100 rad/s. **F**, Normalized velocity magnitude and pathlines on plane 1 (left) and plane 2 (right) for rotating speed 450 rad/s. **G** and **H**, Parameters used to characterize fluctuations and to predict blood damage from turbulence. **G**, Reynolds Shear Stress (RSS) normalized. **H**, Kolmogorov length scale for rotating speed of 450 rad/s.

rotational rates (10, 100, and 450 rad/second) were used as inputs for the simulation and the fluid patterns under each condition. In laminar flow (Figure 4A), the streamlines (shown in gray) are parallel to each other, form a closed path around the vane, and exhibit a highly ordered motion. In transitional flow (Figure 4B), secondary flow patterns can be observed, these consist of converging and diverging separation between adjacent streamlines superimposed on the primary laminar flow. In turbulent flow (Figure 4C), streamlines do not form a closed path and their motion is chaotic. These simulations agree with the experimental results in the vane rheometer (Figure 1C) that show the presence of laminar, transitional, and turbulent flows.

Results on Figure 4D through 4F indicate that maximum velocity occurs at the tip of each blade for all rotating rates. Streamlines (shown in black) show the presence of secondary flows (these are perpendicular to the bulk flow direction) and can be observed in the graphics for all different rotational rates. Vortices (rotating flow), corresponding to secondary flow, can be seen moving from the blade tip toward the wall of the cup as

rotation changes from 10 to 100 rad/second. However, increasing the rotating speed from 100 to 450 rad/second drastically changes the secondary flow pattern and vortices can no longer be observed. Detailed computational fluid dynamics results are shown on [online-only Data Supplement](#).

At 450 rad/second, the flow is turbulent and this phenomenon also adds an additional effective stress to the flow in the form of Reynolds Stress. Reynolds Shear Stress (RSS) is a parameter used to characterize flow fluctuations and to predict blood damage from turbulence.⁶¹ RSS is absent in laminar flow and is a measure of momentum flux in the flow caused by velocity fluctuations. Also, note that RSS is different to wall shear stress, [online-only Data Supplement](#). Results from the simulation show that the RSS is the highest on the faces of the vane (Figure 4G). Finally, the Kolmogorov scale was calculated; the Kolmogorov length scale for the fluid within the cup at a rotational speed of 450 rad/second is shown in Figure 4H. Results from computational fluid dynamic simulations show that at 450 rad/second, the Kolmogorov length scale ranges from 3 to

30 μm depending on the spatial location within the cup and vane. Below this scale, energy from turbulence is completely dissipated by viscosity, on average. Above the Kolmogorov length scale, there are significant velocity fluctuations and transient forces. However, it should be noted that sub-Kolmogorov eddies may exist because of the intermittent instantaneous energy dissipation field.⁶¹ Turbulence at this scale can create instantaneous intense shear stress. However, it is important to mention that the scale is not exact and is instead a theory grounded in the field of turbulence. It provides a relative measure where scales that are larger than the Kolmogorov scale experience turbulent fluctuations, whereas values below the scale do not.

High Shear Stress Alone Is Not Sufficient for VWF Cleavage

From the computational fluid dynamics model, we found that as the rotational rate increases, so does the shear rate, with maximum values occurring near the vane ([online-only Data Supplement](#)). At vane rotational rates of 100 and 450 second^{-1} , the fluid shear rates have a maximum magnitude of 2000 and 6000 second^{-1} adjacent to the surface of the vane. To test the hypothesis that turbulence, and not just high shear stress, is the cause of excessive VWF cleavage, we conducted a set of experiments in a cone-and-plate rheometer under laminar flow conditions. The purified system containing VWF, HSA, and ADAMTS13 was exposed to constant shear rate of 1500, 3000, 3500, 4000, or 6000 second^{-1} for 10 minutes. VWF cleavage as evaluated by western blot (Figure 5A), and multimer analysis (Figure 5B) show

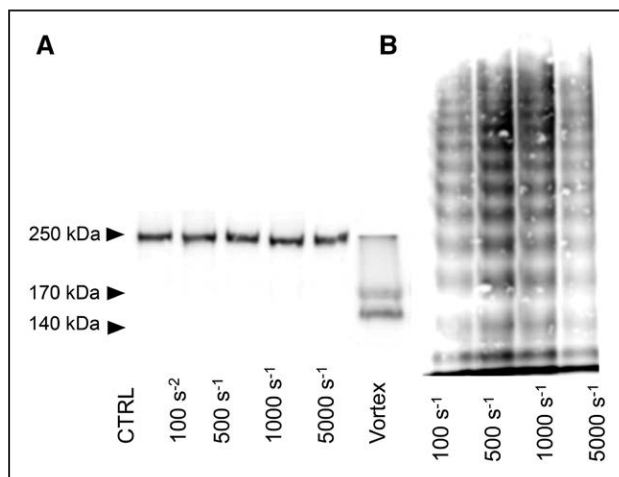


Figure 5. Western blots of VWF (von Willebrand Factor). **A**, VWF cleavage representative of the results obtained with cone-and-plate. All samples contained VWF and ADAMTS13 (a disintegrin and metalloproteinase with a thrombospondin type-1 motif, member 13). Samples in the figure are representative of the samples subjected to constant shear rate for 10 min. **B**, VWF multimer results from cone-and-plate experiments. All samples contained VWF and ADAMTS13. Samples in the figure are representative of the samples subjected to constant shear rate for 10 min. CTRL indicates control.

undetectable cleavage and no significant changes to HMWM. These results indicate that high shear stress under the laminar conditions that we used is not sufficient for soluble VWF to undergo a conformational change that facilitates cleavage by ADAMTS13.

DISCUSSION

Prior studies have used the cone-and-plate rheometer to provide insights into the effects of platelets⁶⁰ and FVIII on cleavage of VWF by ADAMTS13.³⁷ However, the fluid conditions that lead to excessive and pathological cleavage of VWF in AS and MCS are still unknown. Turbulent flow commonly develops in severe AS and in many MCS devices. In patients with severe AS (involving a $\geq 50\%$ reduction in diameter), blood flow can be turbulent at $\text{Re} > 400$.^{62,63} Similarly, most MCS devices present high Re number.⁶⁴ For example, the axial ventricular assist device, Impella (2006) has reported a maximum rotational speed of 50000 rpm and Re of 12566.⁶⁴ The centrifugal ventricular assist device CentriMag has a maximum rotational speed of 5500 rpm and Re of 155320.⁶⁵ Reversal of AVWS occurs post-correction of AS or the removal of the MCS.^{66,67} Altogether, these observations strongly suggest that the excessive cleavage of VWF in AVWS is mediated by nonphysiological flows that occur in both severe AS and MCS.^{68–70} Based on these data, we hypothesized that turbulent flow plays role in excessive cleavage of VWF by ADAMTS13 beyond what is seen by high shear stress. Therefore, we used a vane rheometer to evaluate the effects of laminar, transitional, and turbulent flows on cleavage of full length VWF in the presence of ADAMTS13. Our results show that turbulent flow promotes cleavage of VWF by ADAMTS13 and is likely playing a role in the loss of HMWM observed in AVWS.

Computational fluid dynamics simulations of the vane rheometer provided potential explanations for the effect of nonphysiological flows on VWF cleavage. In turbulent flow, the energy is introduced through larger eddies and is dissipated at the microscopic level through the smallest eddies down to the Kolmogorov length scale. This scale describes the length at which the kinetic energy is dissipated by viscosity.⁷¹ We found that the Kolmogorov scale ranges from 3 to 30 μm at 450 rad/second in the vane rheometer. This scale approaches the size of VWF, reported as 1 to 15 μm depending on the VWF source and conformation.^{11,12} VWF multimers that are higher in size than the Kolmogorov scale could experience large intermittent transient forces. This can result in intense instantaneous shear stress that may expose the A2 domain to ADAMTS13.

The kinetics of loss of HMWM will likely depend on the regions of turbulence within the device and the frequency of exposed VWF to those fluid forces. Loss of HMMW in patients treated with LVADs has been detected as early as after 180 minutes after implantation.⁷² The

residence time VWF spends under turbulent conditions in severe AS or MCS is shorter than the duration of our rheometer experiments. However, the Kolmogorov length scale and RSS is not homogeneously distributed within the rheometer cup. The uneven force distribution significantly reduces the residence time of VWF at a given turbulent condition, making our findings relevant to MCS and severe AS.

Excessive cleavage of VWF in our experiments had functional consequences. VWF exposed to turbulent flow conditions did not support platelet or CB. Interestingly, the VWF sample exposed to transitional flow lacked cleavage fragments on the western blot but showed slightly reduced platelet binding capacity and subtle abnormalities in the multimer composition, represented by lighter staining. These results suggest that VWF binding to GPIIb- α might be affected by transitional flow. Larger VWF multimers possess the greatest hemostatic capacity,^{11,15} but little is known about the progression of cleavage and how it relates to decreased platelet binding function. The slight abnormalities in the multimer pattern of the sample exposed to transitional flow suggest cleavage of VWF that is not detected by western blot. Alternatively, transitional flow could have an effect on the A1 domain of VWF leading to decreased platelet-binding capacity.

Further studies need to be conducted to identify whether other VWF domains are modified by exposure to these fluid regimes. Fluid forces affect VWF, not only by mediating elongation and exposure of the A2 domain but also prior studies have proposed the existence of a metastable active state.⁷³ This state may be considered misfolded because it is a non-native state.⁷⁴ Others have also shown differential binding to a fluorescent probe, post-VWF shear, using fluorescence spectroscopy,⁷⁵ suggesting that the protein undergoes conformational changes because of shear and these might not only facilitate ADAMTS13 cleavage but might also affect the structure of the VWF-A1 platelet-binding domain. Ongoing studies analyzing the VWF-platelet-binding sites changes because of nonphysiological flow conditions will further our understanding of these results.

To evaluate the physiological relevance of our results, we also tested and confirmed that cleavage occurs in the presence of all blood components. However, in whole blood, we cannot rule out other factors that might be playing a role in cleavage. Previous studies suggest that other proteases, such as plasmin, play a role in VWF cleavage.³⁴ Similarly, we did not characterize the unique contribution of platelets in our assay. It has been previously shown that platelets can augment cleavage of VWF,⁶⁰ but secretion of their own VWF hindered our ability to distinguish in a multimer gel between cleaved soluble VWF and platelet VWF. These factors might also affect the kinetics and onset of AVWS in patients.

One of the limitations of our study is that in both the cone-and-plate and vane rheometer, there was protein loss because of adsorption to surfaces as previously reported.^{76,77} However, cleavage of VWF was only identified under turbulent conditions.

In summary, our study shows that turbulent flow conditions facilitate cleavage of VWF, a process mediated by ADAMTS13, rendering VWF functionally deficient. We found that there is a decrease in platelet adhesion on VWF exposed to turbulent flow and VWF activity even before severe structural changes such as loss of HMWM are detected. Our results may have clinical implications for the diagnosis and treatment of AVWS and the manufacturing of MCS.

ARTICLE INFORMATION

Received April 19, 2019; accepted June 10, 2019.

Affiliations

From the Department of Pediatrics (M.B., K.A., F.W., K.B.N., D.B., J.D.P.) and Department of Bioengineering (M.B., K.B.N.), University of Colorado Anschutz Medical Campus, Aurora; Department of Mechanical Engineering (A.S., D.B.) and School of Biomedical Engineering (D.B.), Colorado State University, Fort Collins; and Department of Material Characterization, Thermo Fisher Scientific, Madison, WI (N.C.C.).

Acknowledgments

We thank Katherine Ruegg, MSc, for running the automated latex-enhanced immunoassay (Hemosil, Diagnostica Stago, France) used to determine VWF activity (VWF:Act).

Sources of Funding

This work was supported in part by American Heart Association PreDoctoral Fellowship (18PRE33990253), the National Institutes of Health (R01 HL120728), the National Science Foundation (1762705), and by Career Development Award from the American Heart Association (18CDA34110134).

Disclosures

None.

REFERENCES

1. Savage B, Almus-Jacobs F, Ruggeri ZM. Specific synergy of multiple substrate-receptor interactions in platelet thrombus formation under flow. *Cell*. 1998;94:657–666.
2. Peterson DM, Stathopoulos NA, Giorgio TD, Hellums JD, Moake JL. Shear-induced platelet aggregation requires von willebrand factor and platelet membrane glycoproteins Ib and IIb-IIIa. *Blood*. 1987;69:625–628.
3. Novák L, Deckmyn H, Damjanovich S, Hársfalvi J. Shear-dependent morphology of von willebrand factor bound to immobilized collagen. *Blood*. 2002;99:2070–2076. doi: 10.1182/blood.v99.6.2070
4. Siedlecki CA, Lestini BJ, Kottke-Marchant KK, Eppell SJ, Wilson DL, Marchant RE. Shear-dependent changes in the three-dimensional structure of human von willebrand factor. *Blood*. 1996;88:2939–2950.
5. Kraus E, Kraus K, Obser T, Oyen F, Klemm U, Schneppenheim R, Brehm MA. Platelet-free shear flow assay facilitates analysis of shear-dependent functions of VWF and ADAMTS13. *Thromb Res*. 2014;134:1285–1291. doi: 10.1016/j.thromres.2014.08.013
6. Gogia S, Neelamegham S. Role of fluid shear stress in regulating VWF structure, function and related blood disorders. *Biorheology*. 2015;52:319–335. doi: 10.3233/BIR-15061
7. Nesbitt WS, Mangin P, Salem HH, Jackson SP. The impact of blood rheology on the molecular and cellular events underlying arterial thrombosis. *J Mol Med (Berl)*. 2006;84:989–995. doi: 10.1007/s00109-006-0101-1
8. Sadler JE. Biochemistry and genetics of von willebrand factor. *Annu Rev Biochem*. 1998;67:395–424. doi: 10.1146/annurev.biochem.67.1.395
9. Colace TV, Diamond SL. Direct observation of von willebrand factor elongation and fiber formation on collagen during acute whole blood exposure

- to pathological flow. *Arterioscler Thromb Vasc Biol.* 2013;33:105–113. doi: 10.1161/ATVBAHA.112.300522
10. Jaspe J, Hagen SJ. Do protein molecules unfold in a simple shear flow? *Biophys J.* 2006;91:3415–3424. doi: 10.1529/biophysj.106.089367
 11. Schneider SW, Nuschele S, Wixforth A, Gorzelanny C, Alexander-Katz A, Netz RR, Schneider MF. Shear-induced unfolding triggers adhesion of von willebrand factor fibers. *Proc Natl Acad Sci USA.* 2007;104:7899–7903. doi: 10.1073/pnas.0608422104
 12. Fu H, Jiang Y, Yang D, Scheiflinger F, Wong WP, Springer TA. Flow-induced elongation of von willebrand factor precedes tension-dependent activation. *Nat Commun.* 2017;8:324. doi: 10.1038/s41467-017-00230-2
 13. Majerus EM, Zheng X, Tuley EA, Sadler JE. Cleavage of the ADAMTS13 propeptide is not required for protease activity. *J Biol Chem.* 2003;278:46643–46648. doi: 10.1074/jbc.M309872200
 14. Stocksclaeder M, Schneppenheim R, Budde U. Update on von willebrand factor multimers: focus on high-molecular-weight multimers and their role in hemostasis. *Blood Coagul Fibrinolysis.* 2014;25:206–216. doi: 10.1097/MBC.000000000000065
 15. Zhang X, Halvorsen K, Zhang CZ, Wong WP, Springer TA. Mechanoenzymatic cleavage of the ultralarge vascular protein von willebrand factor. *Science.* 2009;324:1330–1334. doi: 10.1126/science.1170905
 16. Li F, Li CQ, Moake JL, López JA, McIntire LV. Shear stress-induced binding of large and unusually large von willebrand factor to human platelet glycoprotein Ibalph. *Ann Biomed Eng.* 2004;32:961–969.
 17. Zheng XL. ADAMTS13 and von willebrand factor in thrombotic thrombocytopenic purpura. *Annu Rev Med.* 2015;66:211–225. doi: 10.1146/annurev-med-061813-013241
 18. Dong JF, Moake JL, Nolasco L, Bernardo A, Arceneaux W, Shrimpton CN, Schade AJ, McIntire LV, Fujikawa K, López JA. ADAMTS-13 rapidly cleaves newly secreted ultralarge von willebrand factor multimers on the endothelial surface under flowing conditions. *Blood.* 2002;100:4033–4039. doi: 10.1182/blood-2002-05-1401
 19. Federici AB, Mazurier C, Berntorf E, Lee CA, Scharrer I, Goudemand J, Lethagen S, Nitu I, Ludwig G, Hilbert L, Mannucci PM. Biologic response to desmopressin in patients with severe type 1 and type 2 von Willebrand disease: results of a multicenter european study. *Blood.* 2004;103:2032–2038. doi: 10.1182/blood-2003-06-2072
 20. Vincentelli A, Susen S, Le Tourneau T, Six I, Fabre O, Juthier F, Bauters A, Decoene C, Goudemand J, Prat A, Jude B. Acquired von willebrand syndrome in aortic stenosis. *N Engl J Med.* 2003;349:343–349. doi: 10.1056/NEJMoa022831
 21. Van Belle E, Rauch A, Vincentelli A, et al. Von willebrand factor as a biological sensor of blood flow to monitor percutaneous aortic valve interventions. *Circ Res.* 2015;116:1193–1201. doi: 10.1161/CIRCRESAHA.116.305046
 22. Gragnano F, Crisci M, Bigazzi MC, et al. Von willebrand factor as a novel player in valvular heart disease: from bench to valve replacement. *Angiology.* 2018;69:103–112. doi: 10.1177/0003319717708070
 23. Muslem R, Caliskan K, Leebeek FWG. Acquired coagulopathy in patients with left ventricular assist devices. *J Thromb Haemost.* 2017;16:429–440.
 24. Starling RC, Naka Y, Boyle AJ, Gonzalez-Stawinski G, John R, Jorde U, Russell SD, Conte JV, Aaronson KD, McGee EC Jr, Cotts WG, DeNofrio D, Pham DT, Farrar DJ, Pagani FD. Results of the post-U.S. food and drug administration-approval study with a continuous flow left ventricular assist device as a bridge to heart transplantation: a prospective study using the INTERMACS (Interagency Registry for Mechanically Assisted Circulatory Support). *J Am Coll Cardiol.* 2011;57:1890–1898. doi: 10.1016/j.jacc.2010.10.062
 25. Lahpor J, Khaghani A, Hetzer R, Pavie A, Friedrich I, Sander K, Strüber M. European results with a continuous-flow ventricular assist device for advanced heart-failure patients. *Eur J Cardiothorac Surg.* 2010;37:357–361. doi: 10.1016/j.ejcts.2009.05.043
 26. Kirklin JK, Naftel DC, Pagani FD, Kormos RL, Stevenson LW, Blume ED, Myers SL, Miller MA, Baldwin JT, Young JB. Seventh INTERMACS annual report: 15,000 patients and counting. *J Heart Lung Transplant.* 2015;34:1495–1504. doi: 10.1016/j.healun.2015.10.003
 27. Eckman PM, John R. Bleeding and thrombosis in patients with continuous-flow ventricular assist devices. *Circulation.* 2012;125:3038–3047. doi: 10.1161/CIRCULATIONAHA.111.040246
 28. Morishima A, Marui A, Shimamoto T, Saji Y, Tambara K, Nishina T, Komeda M. Successful aortic valve replacement for heyde syndrome with confirmed hematologic recovery. *Ann Thorac Surg.* 2007;83:287–288. doi: 10.1016/j.athoracsur.2006.05.082
 29. Spangenberg T, Budde U, Schewel D, Frerker C, Thielsen T, Kuck KH, Schäfer U. Treatment of acquired von willebrand syndrome in aortic stenosis with transcatheter aortic valve replacement. *JACC Cardiovasc Interv.* 2015;8:692–700. doi: 10.1016/j.jcin.2015.02.008
 30. Yamashita K, Yagi H, Hayakawa M, Abe T, Hayata Y, Yamaguchi N, Sugimoto M, Fujimura Y, Matsumoto M, Taniguchi S. Rapid restoration of thrombus formation and high-molecular-weight von willebrand factor multimers in patients with severe aortic stenosis after valve replacement. *J Atheroscler Thromb.* 2016;23:1150–1158. doi: 10.5551/jat.34421
 31. Crawley JT, de Groot R, Xiang Y, Luken BM, Lane DA. Unraveling the scissile bond: how ADAMTS13 recognizes and cleaves von willebrand factor. *Blood.* 2011;118:3212–3221. doi: 10.1182/blood-2011-02-306597
 32. Singh I, Themistou E, Porcar L, Neelamegham S. Fluid shear induces conformation change in human blood protein von willebrand factor in solution. *Biophys J.* 2009;96:2313–2320. doi: 10.1016/j.bpj.2008.12.3900
 33. Cao W, Krishnaswamy S, Camire RM, Lenting PJ, Zheng XL. Factor VIII accelerates proteolytic cleavage of von Willebrand factor by ADAMTS13. *Proc Natl Acad Sci USA.* 2008;105:7416–7421. doi: 10.1073/pnas.0801735105
 34. Brophy TM, Ward SE, McGimsey TR, Schneppenheim S, Drakeford C, O'Sullivan JM, Chion A, Budde U, O'Donnell JS. Plasmin cleaves von willebrand factor at K1491-R1492 in the A1-A2 linker region in a shear- and glycan-dependent manner *in vitro*. *Arterioscler Thromb Vasc Biol.* 2017;37:845–855. doi: 10.1161/ATVBAHA.116.308524
 35. Zhang P, Pan W, Rux AH, Sachais BS, Zheng XL. The cooperative activity between the carboxyl-terminal TSP1 repeats and the CUB domains of ADAMTS13 is crucial for recognition of von willebrand factor under flow. *Blood.* 2007;110:1887–1894. doi: 10.1182/blood-2007-04-083329
 36. Anderson PJ, Kokame K, Sadler JE. Zinc and calcium ions cooperatively modulate ADAMTS13 activity. *J Biol Chem.* 2006;281:850–857. doi: 10.1074/jbc.M504540200
 37. Skipwith CG, Cao W, Zheng XL. Factor VIII and platelets synergistically accelerate cleavage of von willebrand factor by ADAMTS13 under fluid shear stress. *J Biol Chem.* 2010;285:28596–28603. doi: 10.1074/jbc.M110.131227
 38. White FM. *Viscous Fluid Flow*. New York, NY: McGraw-Hill; 1991.
 39. Yunus A, Cengel D, Cimbala JM. *Fluid Mechanics Fundamentals and Applications*. New York, NY: McGraw-Hill Education; 2013.
 40. McCormick SM, Seil JT, Smith DS, Tan F, Loth F. Transitional flow in a cylindrical flow chamber for studies at the cellular level. *Cardiovasc Eng Technol.* 2012;3:439–449. doi: 10.1007/s13239-012-0107-5
 41. Coulter NA Jr, Pappenheimer JR. Development of turbulence in flowing blood. *Am J Physiol.* 1949;159:401–408. doi: 10.1152/ajplegacy.1949.159.2.401
 42. Al-Azawy MG, Turan A, Revell A. Investigating the impact of non-Newtonian blood models within a heart pump. *Int J Numer Method Biomed Eng.* 2017;33:e02780.
 43. Al-Azawy MG, Turan A, Revell A. In: Lacković I, Vasic D, eds. *Investigating the Use of Turbulence Models for Flow Investigations in a Positive Displacement Ventricular Assist Device BT - 6th European Conference of the International Federation for Medical and Biological Engineering*. Cham, Switzerland: Springer International Publishing; 2015:395–398.
 44. Nishio K, Anderson PJ, Zheng XL, Sadler JE. Binding of platelet glycoprotein Ibalph to von willebrand factor domain A1 stimulates the cleavage of the adjacent domain A2 by ADAMTS13. *Proc Natl Acad Sci USA.* 2004;101:10578–10583. doi: 10.1073/pnas.0402041101
 45. Zhang Q, Gao B, Chang Y. The study on hemodynamic effect of series type LVAD on aortic blood flow pattern: a primary numerical study. *Biomed Eng Online.* 2016;15(suppl 2):163. doi: 10.1186/s12938-016-0252-4
 46. Turan A, Revell A. Assessment of turbulence models for pulsatile flow inside a heart pump AU - Al-Azawy, Mohammed G. *Comput Methods Biomech Biomed Engin.* 2016;19:271–285.
 47. Zhang C, Neelamegham S. Application of microfluidic devices in studies of thrombosis and hemostasis. *Platelets.* 2017;28:434–440. doi: 10.1080/09537104.2017.1319047
 48. Kawanami O, Jin E, Ghazizadeh M, Fujiwara M, Jiang L, Nagashima M, Shimizu H, Takemura T, Ohaki Y, Arai S, Gombuchui M, Takeda K, Yu ZX, Ferrans VJ. Heterogeneous distribution of thrombomodulin and von Willebrand factor in endothelial cells in the human pulmonary microvessels. *J Nippon Med Sch.* 2000;67:118–125.
 49. Onasoga-Jarvis AA, Leiderman K, Fogelson AL, Wang M, Manco-Johnson MJ, Di Paola JA, Neeves KB. The effect of factor VIII deficiencies and replacement and bypass therapies on thrombus formation under venous flow conditions in microfluidic and computational models. *PLoS One.* 2013;8:e78732. doi: 10.1371/journal.pone.0078732
 50. Ng CJ, McCrae KR, Ashworth K, Sosa LJ, Betapudi V, Manco-Johnson MJ, Liu A, Dong JF, Chung D, White-Adams TC, López JA, Di Paola J. Effects of anti-β2GPI antibodies on VWF release from human umbilical vein

- endothelial cells and ADAMTS13 activity. *Res Pract Thromb Haemost* 2018;2:380–389. doi: 10.1002/rth2.12090
51. Kokame K, Nobe Y, Kokubo Y, Okayama A, Miyata T. FRETS-VWF73, a first fluorogenic substrate for ADAMTS13 assay. *Br J Haematol*. 2005;129:93–100. doi: 10.1111/j.1365-2141.2005.05420.x
 52. Han Y, Xiao J, Falls E, Zheng XL. A shear-based assay for assessing plasma ADAMTS13 activity and inhibitors in patients with thrombotic thrombocytopenic purpura. *Transfusion*. 2011;51:1580–1591. doi: 10.1111/j.1537-2995.2010.03020.x
 53. White-Adams TC, Ng CJ, Jacobi PM, Haberichter SL, Di Paola JA. Mutations in the D'D3 region of VWF traditionally associated with type 1 VWD lead to quantitative and qualitative deficiencies of VWF. *Thromb Res*. 2016;145:112–118. doi: 10.1016/j.thromres.2016.08.009
 54. Crawford NC, Sprague MA, Stickel JJ. Mixing behavior of a model cellulosic biomass slurry during settling and resuspension. *Chem Eng Sci*. 2016;144:310–320.
 55. Dent JA, Berkowitz SD, Ware J, Kasper CK, Ruggeri ZM. Identification of a cleavage site directing the immunochemical detection of molecular abnormalities in type IIA von willebrand factor. *Proc Natl Acad Sci USA*. 1990;87:6306–6310. doi: 10.1073/pnas.87.16.6306
 56. Dent JA, Galbusera M, Ruggeri ZM. Heterogeneity of plasma von willebrand factor multimers resulting from proteolysis of the constituent subunit. *J Clin Invest*. 1991;88:774–782. doi: 10.1172/JCI115376
 57. Budde U, Schneppenheim R, Eikenboom J, et al. Detailed von willebrand factor multimer analysis in patients with von willebrand disease in the european study, molecular and clinical markers for the diagnosis and management of type 1 von willebrand disease (MCMDM-1VWD). *J Thromb Haemost*. 2008;6:762–771.
 58. Budde U, Drewke E, Mainus K, Schneppenheim R. Laboratory diagnosis of congenital von willebrand disease. *Semin Thromb Hemost*. 2002;28:173–190. doi: 10.1055/s-2002-27820
 59. Geisen U, Brehm K, Trummer G, et al. Platelet secretion defects and acquired von willebrand syndrome in patients with ventricular assist devices. *J Am Heart Assoc*. 2018;7:e006519.
 60. Shim K, Anderson PJ, Tuley EA, Wiswall E, Sadler JE. Platelet-VWF complexes are preferred substrates of ADAMTS13 under fluid shear stress. *Blood*. 2008;111:651–657. doi: 10.1182/blood-2007-05-093021
 61. Morshed KN, Bark D Jr, Forleo M, Dasi LP. Theory to predict shear stress on cells in turbulent blood flow. *PLoS One*. 2014;9:e105357. doi: 10.1371/journal.pone.0105357
 62. Al-Azawy MG, Turan A, Revell A. Assessment of turbulence models for pulsatile flow inside a heart pump. *Comput Methods Biomech Biomed Engin*. 2016;19:271–285. doi: 10.1080/10255842.2015.1015527
 63. Ha H, Lee SJ. Effect of swirling inlet condition on the flow field in a stenosed arterial vessel model. *Med Eng Phys*. 2014;36:119–128. doi: 10.1016/j.medengphy.2013.10.008
 64. Fraser KH, Taskin ME, Griffith BP, Wu ZJ. The use of computational fluid dynamics in the development of ventricular assist devices. *Med Eng Phys*. 2011;33:263–280. doi: 10.1016/j.medengphy.2010.10.014
 65. De Robertis F, Birks EJ, Rogers P, Dreyfus G, Pepper JR, Khaghani A. Clinical performance with the levitronix centrimag short-term ventricular assist device. *J Heart Lung Transplant*. 2006;25:181–186. doi: 10.1016/j.healun.2005.08.019
 66. Frank RD, Lanzmich R, Haager PK, Budde U. Severe aortic valve stenosis. *Clin Appl Thromb Hemost*. 2017;23:229–234. doi: 10.1177/1076029616660759
 67. Loeffelbein F, Funk D, Nakamura L, Zieger B, Grohmann J, Siepe M, Kroll J, Stiller B. Shear-stress induced acquired von Willebrand syndrome in children with congenital heart disease. *Interact Cardiovasc Thorac Surg*. 2014;19:926–932. doi: 10.1093/icvts/ivu305
 68. Meyer AL, Malehsa D, Budde U, Bara C, Haverich A, Strueber M. Acquired von willebrand syndrome in patients with a centrifugal or axial continuous flow left ventricular assist device. *JACC Heart Fail*. 2014;2:141–145. doi: 10.1016/j.jchf.2013.10.008
 69. Chen D, Thomas CS, Blackshear JL. Predictors of acquired von willebrand syndrome in patients with aortic stenosis. *Blood*. 2015;118:3318.
 70. Heilmann C, Trummer G, Beyersdorf F, Brehm K, Berchtold-Herz M, Schelling J, Geisen U, Zieger B. Acquired von willebrand syndrome in patients on long-term support with HeartMate II. *Eur J Cardiothorac Surg*. 2017;51:587–590. doi: 10.1093/ejcts/ezw348
 71. Schüle CY, Affeld K, Kossatz M, Paschereit CO, Kertzsch U. Turbulence measurements in an axial rotary blood pump with laser doppler velocimetry. *Int J Artif Organs*. 2017;40:109–117.
 72. Eric VB, Antoine R, André V, et al. von Willebrand factor as a biological sensor of blood flow to monitor percutaneous aortic valve interventions. *Circ Res*. 2015;116:1193–1201.
 73. Wijeratne SS, Botello E, Yeh HC, Zhou Z, Bergeron AL, Frey EW, Patel JM, Nolasco L, Turner NA, Moake JL, Dong JF, Kiang CH. Mechanical activation of a multimeric adhesive protein through domain conformational change. *Phys Rev Lett*. 2013;110:108102. doi: 10.1103/PhysRevLett.110.108102
 74. Sali A, Shakhnovich E, Karplus M. How does a protein fold? *Nature*. 1994;369:248–251. doi: 10.1038/369248a0
 75. Themistou E, Singh I, Shang C, Balu-lyer SV, Alexandridis P, Neelamegham S. Application of fluorescence spectroscopy to quantify shear-induced protein conformation change. *Biophys J*. 2009;97:2567–2576. doi: 10.1016/j.bpj.2009.08.023
 76. Choi H, Aboufatova K, Pownall HJ, Cook R, Dong JF. Shear-induced disulfide bond formation regulates adhesion activity of von willebrand factor. *J Biol Chem*. 2007;282:35604–35611. doi: 10.1074/jbc.M704047200
 77. Chung DW, Chen J, Ling M, Fu X, Blevins T, Parsons S, Le J, Harris J, Martin TR, Konkle BA, Zheng Y, López JA. High-density lipoprotein modulates thrombosis by preventing von willebrand factor self-association and subsequent platelet adhesion. *Blood*. 2016;127:637–645. doi: 10.1182/blood-2014-09-599530